Supporting Information (SI) Appendix

Membrane protein structure determination by SAD, SIR, or SIRAS phasing in serial femtosecond crystallography using an iododetergent

Authors: Takanori Nakane, Shinya Hanashima, Mamoru Suzuki, Haruka Saiki, Taichi Hayashi, Keisuke Kakinouchi, Shigeru Sugiyama, Satoshi Kawatake, Shigeru Matsuoka, Nobuaki Matsumori, Eriko Nango, Jun Kobayashi, Tatsuro Shimamura, Kanako Kimura, Chihiro Mori, Naoki Kunishima, Michihiro Sugahara, Yoko Takakyu, Shigeyuki Inoue, Tetsuya Masuda, Toshiaki Hosaka, Kensuke Tono, Yasumasa Joti, Takashi Kameshima, Takaki Hatsui, Makina Yabashi, Tsuyoshi Inoue, Osamu Nureki, So Iwata, Michio Murata, and Eiichi Mizohata

1. Supplementary Materials and Methods

1.1. Determination of critical micelle concentration (CMC). The pyrene 1:3 method (1) was employed to estimate the CMC of HAD13a. n-Dodecyl-β-D-maltopyranoside (DDM; Anatrace D310) was used for control experiments, because it is one of the most frequently used detergent in membrane protein crystallography. Graded concentration series of HAD13a and DDM were prepared using saturated pyrene solution (ca. 0.7 μM) in distilled water. Fluorescence of pyrene was measured using a JASCO FP6500 spectrofluorometer (Tokyo, Japan) at 25 °C. The excitation wavelength of pyrene was set to 335 nm with scanning the emission wavelength in the range 360–400 nm. The intensity ratio of the first and third vibronic bands (I_1/I_3) located at around 373 nm (I_1) and 384 nm (I_3) was determined for each concentration of HAD13a and DDM. According to the procedure of Aguiar *et al*. (1), the CMC for the mild detergent HAD13a was determined from the intersection of the straight lines (Fig. S1A), while that for the strong detergent DDM was determined from the inflection point of the sigmoidal curve (Fig. S1B).

1.2. Crystallization of bR in bicelles. Purple membranes from *Halobacterium salinarumstrain* R1M1 were prepared according to a standard method (2). The concentration of bR in the purple membranes was adjusted to 9.0 mg/mL in 2 mM HEPES-NaOH buffer (pH 7.0) containing 20 mM NaCl and 0.01%(w/v) NaN_3. To prepare 25%(w/v) DMPC/CHAPSO bicelles, 25 mg 1,2-dimyristoyl-sn-glycero-3-phosphocholine (DMPC) (Avanti) was mixed with 83.3 μL 10%(w/v) 3-[(3-cholamidopropyl)dimethylammonio]-2-hydroxypropanesulfonate (CHAPSO) (Sigma-Aldrich) and 10 μL water, and incubated at 40 °C for 5 min. The purple membranes and the DMPC/CHAPSO bicelles were mixed in a 4:1 ratio and incubated for 30 min at 0 °C in the dark. In a 1.5-mL microtube, 20 μL sample was mixed with 20 μL precipitant solution [3.2 M NaH_2PO_4, 3.5%(w/v) triethylene glycol and 180 mM 1,6-hexanediol], and another 100 μL precipitant solution was gently added under the mixture at the bottom of the tube, which gave a two-phase solution. The sample was placed at 27 °C in the dark, and large crystals appeared in 1 day. Seeding solution was prepared by sonicating the large crystals with a UD-211 Ultrasonicator (Tomy). Microcrystals for SFX were grown by the rotational crystallization technique using seeds of bR. In 2.0-mL microtubes, 20 μL bicelles containing bR were mixed with 120 μL precipitant solution, and 2 μL seeding solution was added. The microtubes were placed on an RT-50 Rotator (TAITEC) at 18 rpm and 20 °C for 2 days. Sizes of the microcrystals were between 10 and 70 μm as observed using the digital microscope KH-8700 (Hirox). For preparation of heavy-atom derivative crystals, HAD13a, I3C or $BaCl_2$ was added into the tube at a final concentration of 4 mM and incubated with rotation for an additional 3 days.

1.3. SFX data collection for bR. Just before data collection, the microcrystals of bR were mixed with a grease matrix, Synthetic Grease Super Lube (21030; SyncoChemical), and packed in an

injector syringe (nozzle diameter: 110 μm) for native bR as described previously (3), whereas for heavy-atom derivatives, another type of injector syringe (150 μm), which was developed based on the design of the LCP injector reported by Weierstall et al. (4), was used. The new injector, consisting of a hydraulic cylinder, a removable sample reservoir and a nozzle, was installed in the chamber, and the temperature of the injector was kept constant at 20 °C by water circulation. Diffraction patterns were collected at beamline BL3(EH4) of SACLA (5) using the multi-port charge-coupled device (MPCCD) detector (6). The injector was installed in a diffraction chamber enclosure DAPHNIS (7). The sample chamber was filled with helium gas and maintained at 20 °C with humidity of 70–99%. The flow rate was set to 0.25 μL/min (439 μm/s) for native bR and 0.95 μL/min (896 μm/s) for heavy-atom derivatives. The microcrystals were exposed to single XFEL pulses with a photon energy of 7.0 keV, a duration of 2–10 fs and a repetition rate of 30 Hz. The XFEL pulses consisted of 3.6×10^{10} photons per pulse focused to 1.2 (height) × 2.4 μm (width) for native bR and 2.1×10^{11} photons per pulse focused to 1.4 × 1.7 μm for heavy-atom derivatives at the interaction point using Kirkpatrick–Baez mirrors. The typical pulse energy at the sample was 40 μJ per pulse for native bR and 240 μJ per pulse for heavy-atom derivatives. Data collection was guided by real time analysis by the *Cheetah* pipeline adapted for SACLA (8).

1.4. Purification of bR. Delipidation and purification of bR were performed as previously described (9) with some modifications. A suspension of the purple membrane (100 mg of bacteriorhodopsin) was ultracentrifuged at 100,000 × *g* for 20 min at 4 °C. The pellet was resuspended in 5 mL of 10 mM Tris-HCl buffer (pH 7.0) containing 5%(v/v) Triton X-100 and the mixture was allowed to stand, with occasional vigorous agitation, in the dark at 25 °C for 2 days. The solution was centrifuged at 50,000 × *g* for 15 min at 4 °C, and the supernatant was applied to a HiLoad 16/600 Superdex 75 pg column (GE Healthcare) that had been equilibrated with 20 mM Tris-HCl buffer (pH 8.0) containing 150 mM NaCl and 0.25%(w/v) sodium deoxycholate (Sigma). The column was eluted with the equilibration buffer at 4 °C, and fractions containing delipidated bacteriorhodopsin were collected. The sample was concentrated to 4.46 mg/mL with a 30 kD molecular weight cutoff Vivaspin 20 concentrator (Sartorius), frozen in liquid nitrogen, and stored at −80 °C until use in SEC-TS assays. The protein concentration was determined spectrophotometrically based on absorbance at 280 nm (A_{280}), calculated by (A_{280}/3.10) mg/mL.

1.5. Expression and purification of A2a-BRIL. DNA encoding A2a-BRIL was synthesized by Genscript. The gene contains an insertion of a thermostabilized apocytochrome b_{562}RIL (BRIL) from *Escherichia coli* between residues Lys209 and Gly218 in the intracellular loop 3 region of the A2a adenosine receptor, and a truncation of the C-terminal residues 317-412, as published previously (Liu *et al.* 2012). The gene also contains a N154Q mutation to eliminate the glycosylation site. For expression, a modified pFastBac1 vector (Invitrogen) was used, which had a hemagglutinin signal sequence followed by a FLAG tag at the N-terminus and a 10×His tag at

the C-terminus. The A2a-BRIL DNA was inserted into the vector using an In-Fusion HD Cloning Kit (Clontech).

The A2a-BRIL protein was expressed using an Sf9 insect cell-baculovirus system. Cells were grown at 27 °C in ESF921 medium (Expression Systems) including 2% fetal bovine serum (Biowest), 0.5% penicillin-streptomycin (Wako) and 0.5 μg/mL Amphotericin B (Wako). High-titer recombinant baculovirus (>10^8 plaque forming units/mL) was obtained using the Bac-to-Bac Baculovirus Expression System (Invitrogen), according to the manufacturer's protocol. Sf9 cells at a density of ~2 × 10^6 cells/mL were infected with a multiplicity of infection (MOI) of 3. Cells were harvested 48 h postinfection and stored at −80 °C in phosphate buffered saline (PBS) containing 10%(v/v) glycerol.

Insect cell membranes were isolated and purified as described previously (10). Purified membranes were resuspended in 50 mM HEPES buffer (pH 7.5) containing 0.8 M NaCl and 10% glycerol, and stored at −80 °C until use. Purification of A2a-BRIL in complex with ZM241385 from cell membranes was performed as described in reference (10) by using batch purification instead of gravity-flow column. After the purification, the protein was concentrated to ca. 50 mg/mL with a 100-kD molecular weight cutoff Amicon concentrator (Millipore). The protein concentration was estimated using a Pierce BCA Protein Assay Kit (Thermo Fisher Scientific).

1.6. SEC-TS assay. The size-exclusion chromatography-based thermostability (SEC-TS) assay (11, 12) was carried out using purified bR (Fig. S2) and A2a-BRIL (Fig. S3). For bR, aliquots of 624 μg (233 μL) were prepared in 20 mM Tris-HCl buffer (pH 8.0) containing 150 mM NaCl and 0.25% sodium deoxycholate as a control. Other aliquots containing additional detergent 4 mM HAD13a or 4 mM n-nonyl-β-D-maltopyranoside (NM; Anatrace N330) in the same buffer were also prepared to evaluate the effect of the detergents on the thermostability of bR. The samples were incubated at different temperatures for 10 min in a block incubator (Astec). Following ultracentrifugation at 100,000 × *g* for 30 min to remove aggregates, the supernatant (200 μL) was injected into a Superose 6 10/300 GL (GE Healthcare) column on an AKTA purifier (GE Healthcare). The column was eluted with 20 mM Tris-HCl buffer (pH 8.0) containing 150 mM NaCl and 0.25% sodium deoxycholate at a flow rate of 0.50 mL/min.

For A2a-BRIL, 167 μg (117 μL) control aliquots were prepared in 25 mM HEPES-NaOH buffer (pH 7.5) containing 0.8 M NaCl, 10 % glycerol, 250 mM imidazole, 0.02% DDM and 0.71 μM ZM241385. Other aliquots containing additional detergent 4 mM HAD13a in the same buffer were prepared to evaluate the effect of HAD13a on A2a-BRIL. The samples were incubated at different temperatures for 10 min in a block incubator. After ultracentrifugation at 100,000 × *g* for 30 min, the supernatant (100 μl) was applied to the Superose 6 10/300 GL column. The column was eluted with 25 mM HEPES-NaOH buffer (pH 7.5) containing 0.8 M NaCl, 10 % glycerol, 250 mM imidazole and 0.02% DDM at a flow rate of 0.37 mL/min. Melting curves were obtained by plotting normalized peak heights from SEC against temperature.

1.7. Crystallization of A2a-BRIL in LCP. Microcrystals of A2a-BRIL in complex with ZM241385 were obtained in lipidic cubic phases (LCP). The protein solution was reconstituted into LCP by mixing with molten lipid using Hamilton syringes connected with a syringe coupler (13). The protein-LCP mixture contained 40%(w/w) protein solution, 54%(w/w) monoolein (Sigma), and 6%(w/w) cholesterol (Sigma). We grew the crystals by using an original crystallization method with a thin metal wire. The detailed protocol will be published elsewhere. Briefly, after reconstitution into LCP, the syringe and coupler were removed, and a cleaning wire ca. 1.5 cm long was inserted into the protein-laden LCP so as to retain a straight column. The protein-laden LCP was extruded from a syringe into a 0.2-mL PCR tube and soaked in precipitant solution containing 27%(v/v) PEG400, 50 mM sodium thiocyanate, 2%(v/v) 2,5-hexanediol, and 100 mM sodium citrate (pH 5.0), followed by incubation at 20 °C. A shower of small crystals appeared within a week. The LCP with crystals was transferred into a syringe and then gently mixed with molten monoolein containing 40 mM HAD13a to a final concentration of 12 mM HAD13a by using syringes and a syringe coupler. The mixture was incubated at 20 °C for several days in a syringe. Before SFX data collection, monoolein was added to the LCP with crystals to absorb the precipitant and homogenize at approximately 20% of the final volume. The protein samples were loaded into the LCP injector thorough a 400-μm internal diameter (i.d.) nozzle.

1.8. SFX data collection and structure determination of A2a-BRIL. Data collection was performed at beamline BL3(EH4) of SACLA (5) using 7.0 keV XFEL with a pulse duration of 2–10 fs and a repetition rate of 30 Hz. The LCP injector was installed in the diffraction chamber (7) filled with helium gas. A vacuum cleaning device was placed immediately below the injector. Diffraction patterns were recorded on the MPCCD detector (6) with a sample-to-detector distance of 50 mm. The microcrystals of A2a-BRIL soaked with HAD13a were extruded through a 75 or 100 μm i.d. nozzle at a flow rate of 0.24 or 0.42 μL/min, respectively. Data collection was guided by real time analysis by the *Cheetah* pipeline adapted for SACLA (8).

Using the *Cheetah* pipeline, raw images were retrieved from SACLA API (14) and filtered by *Cheetah* (15). Algorithm 6 in *Cheetah* was used for hit finding. Images with more than 20 spots were retained as hits and converted to the HDF5 format for subsequent processing in *CrystFEL* (0.6.2) (16). Detector metrology was refined by *geoptimiser* and *detector-shift* in the *CrystFEL* suite. Indexing was performed by *DirAx* (17). Spot finding was performed by the built-in spot finder (18) in *CrystFEL* with threshold 400, minimum gradient 200,000 and minimum signal-to-noise ratio 5. All datasets were indexed in space group $C222_1$. The mean unit cell parameters were a = 40.19, b = 179.52 and c = 142.13 Å. The radii of the integration and background masks were 3 and 7, respectively. Intensities were merged by *process_hkl* in the *CrystFEL* suite with linear scaling (*--scale option*). No per-image resolution cutoff and no saturation cutoff were employed.

The structure of the HAD13a-derivatized A2a-BRIL was determined by the molecular

replacement method using *Phaser* (19) with a reported A2a-BRIL structure (PDB ID: 4EIY) (10) as the search model, because trials of SAD phasing failed. Manual model fitting was carried out in *Coot* (20). Structural refinement was performed using *Refmac5* (21) in the *CCP4* suite (22). Anomalous difference maps were calculated with *ANODE* (23) to 2.7 Å using final refined models as the phase source. Protein structures were drawn with *PyMOL* (version 1.5.0.4) (https://www.pymol.org). Data statistics are summarized in Table S1.

2. SI Figures

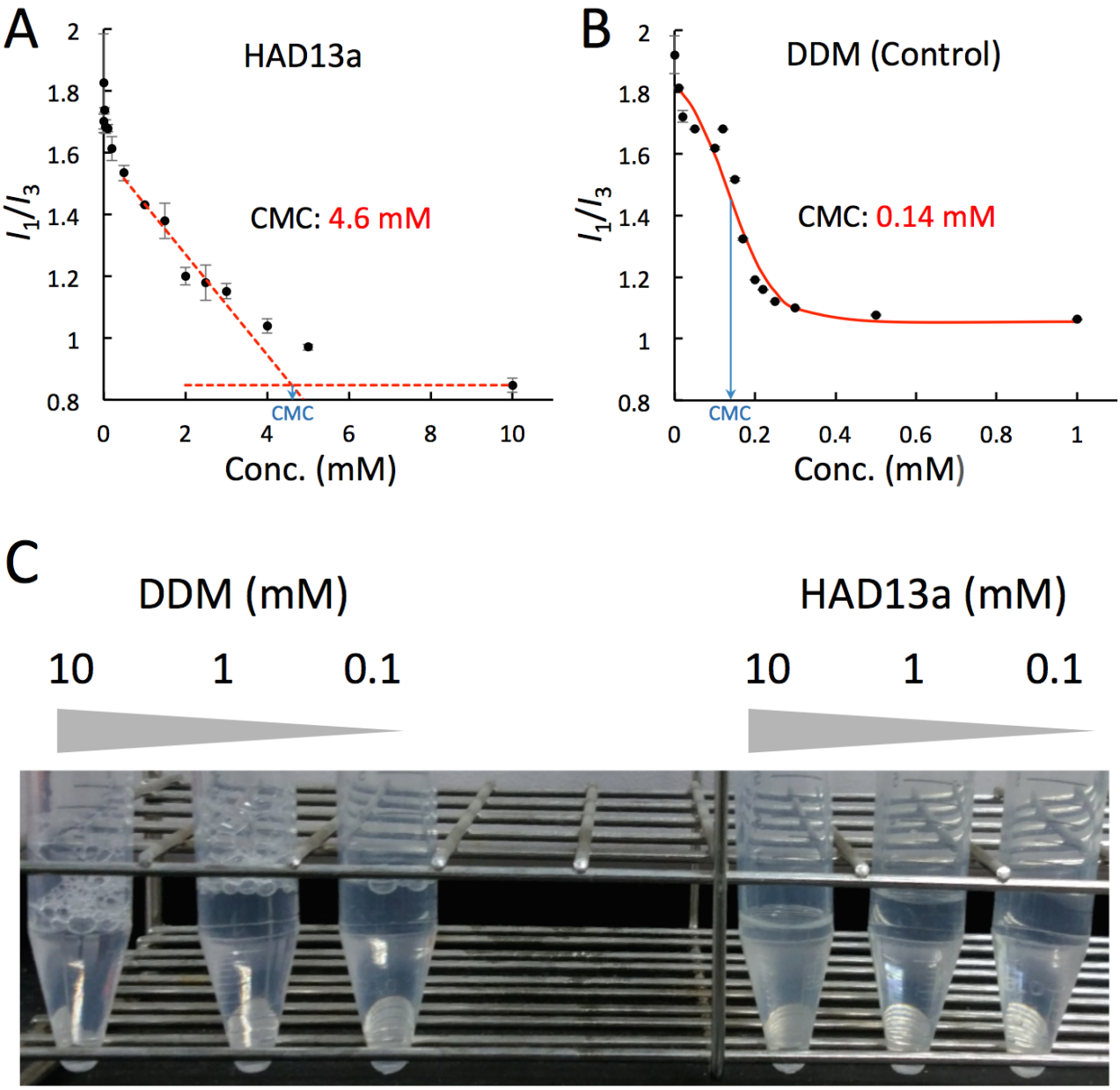

Fig. S1. Measurement of the CMC of HAD13a and DDM by the pyrene 1:3 ratio method (1). Plots of pyrene 1:3 ratio (I_1/I_3) versus concentration of HAD13a (A) are shown in comparison with DDM (B); the CMC of DDM was in good agreement with the reported value of 0.17 mM (24). Test tubes containing solutions of DDM or HAD13a were briefly shaken and the foaming properties of the detergents were evaluated (C).

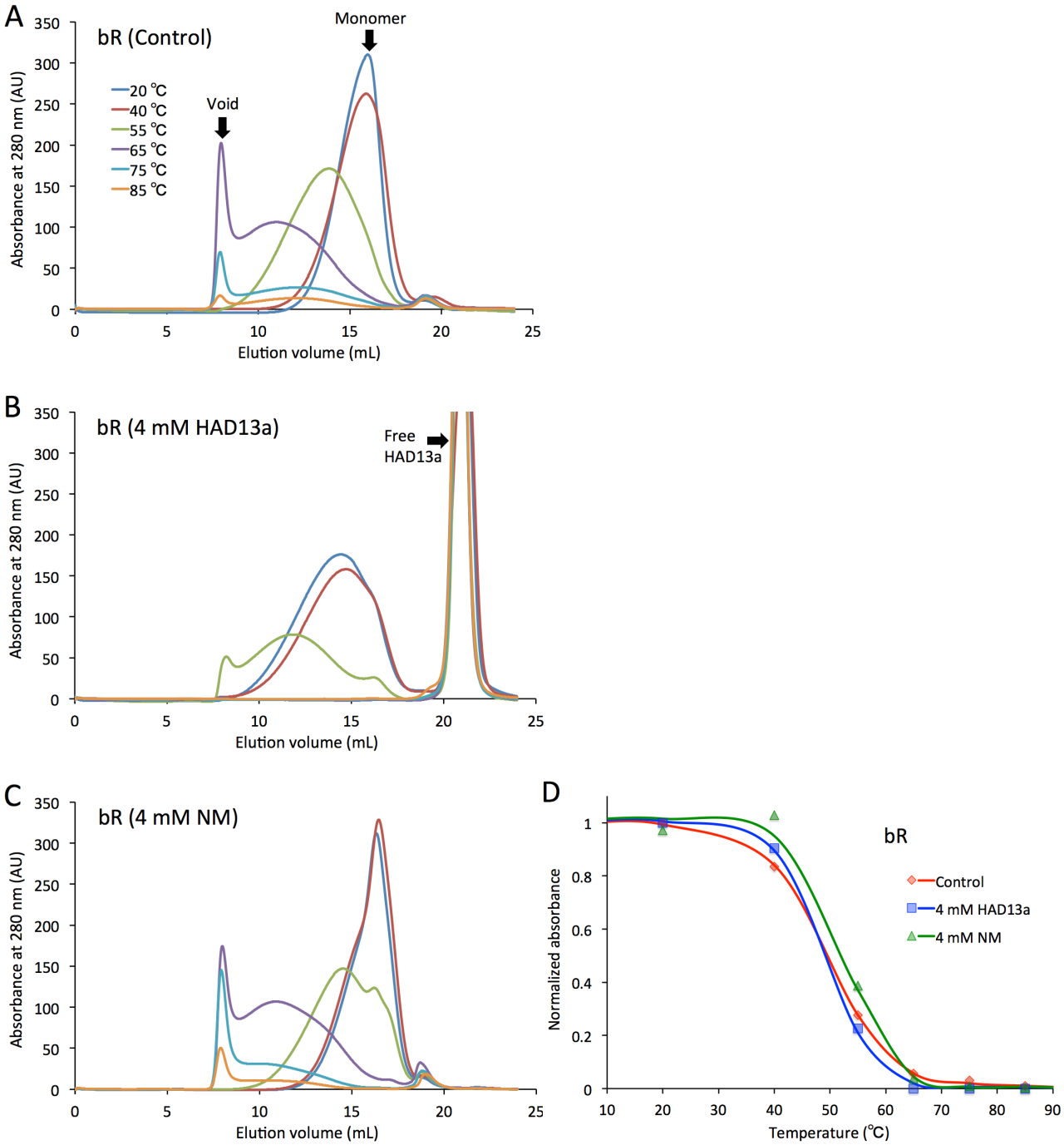

Fig. S2. Effect of HAD13a or NM on thermostability of bR, evaluated by the SEC-TS assay (11, 12). Purified bR sample without additional detergent (as a control) (A) and that supplemented with 4 mM HAD13a (B) or 4 mM NM (C) was incubated for 10 min at the indicated temperatures, centrifuged to remove sold material, injected onto the Superose 6 column, and detected by UV absorbance at 280 nm. Melting curves were drawn by plotting normalized SEC peak heights against temperature (D).

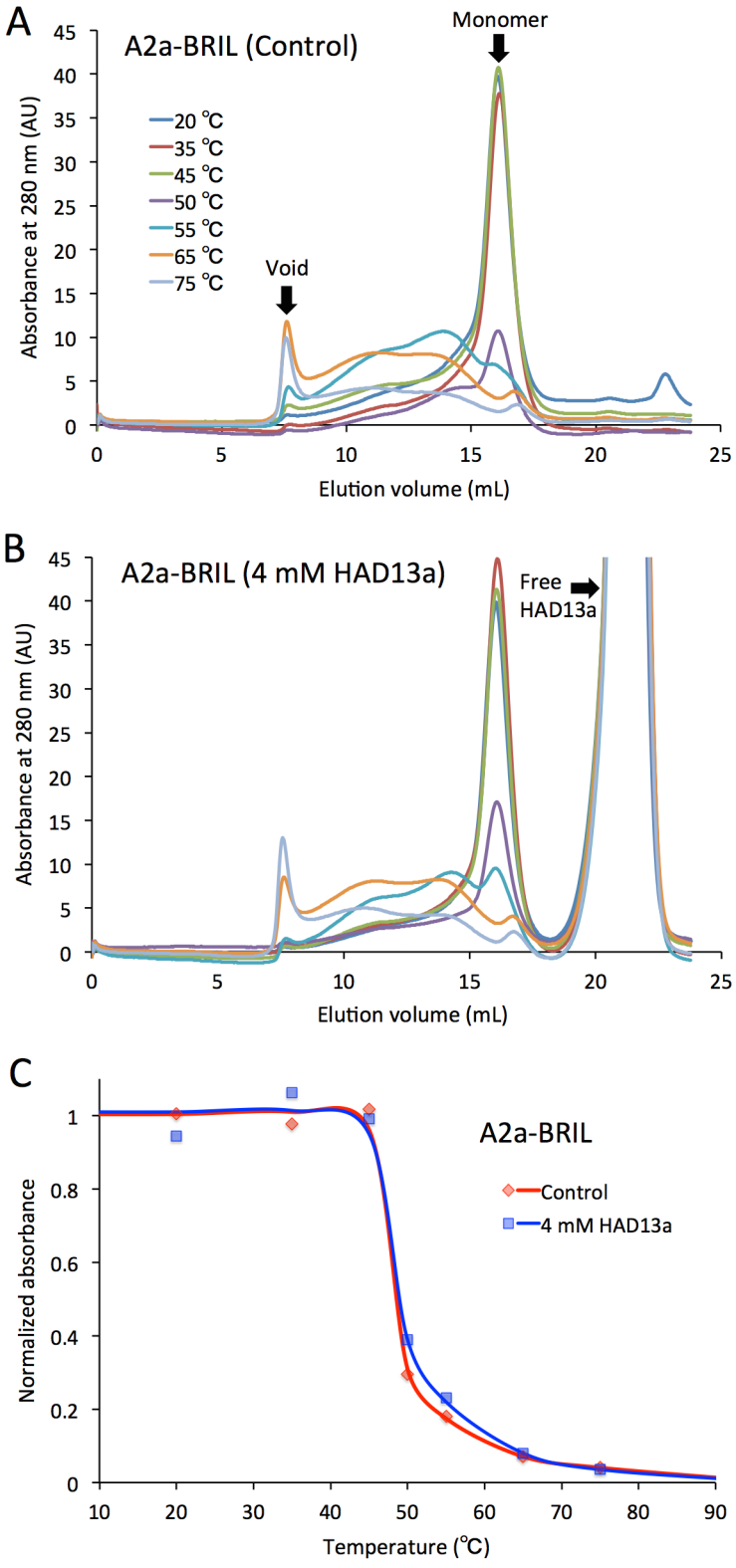

Fig. S3. Effect of HAD13a on thermostability of A2a-BRIL, evaluated by the SEC-TS assay (11, 12). Purified A2a-BRIL sample without additional detergent (as a control) (A) and that supplemented with 4 mM HAD13a (B) was incubated for 10 min at the depicted temperatures, centrifuged, injected onto the Superose 6 column, and detected by UV absorbance at 280 nm. Melting curves were drawn by plotting peak heights of recovered samples against temperature (C).

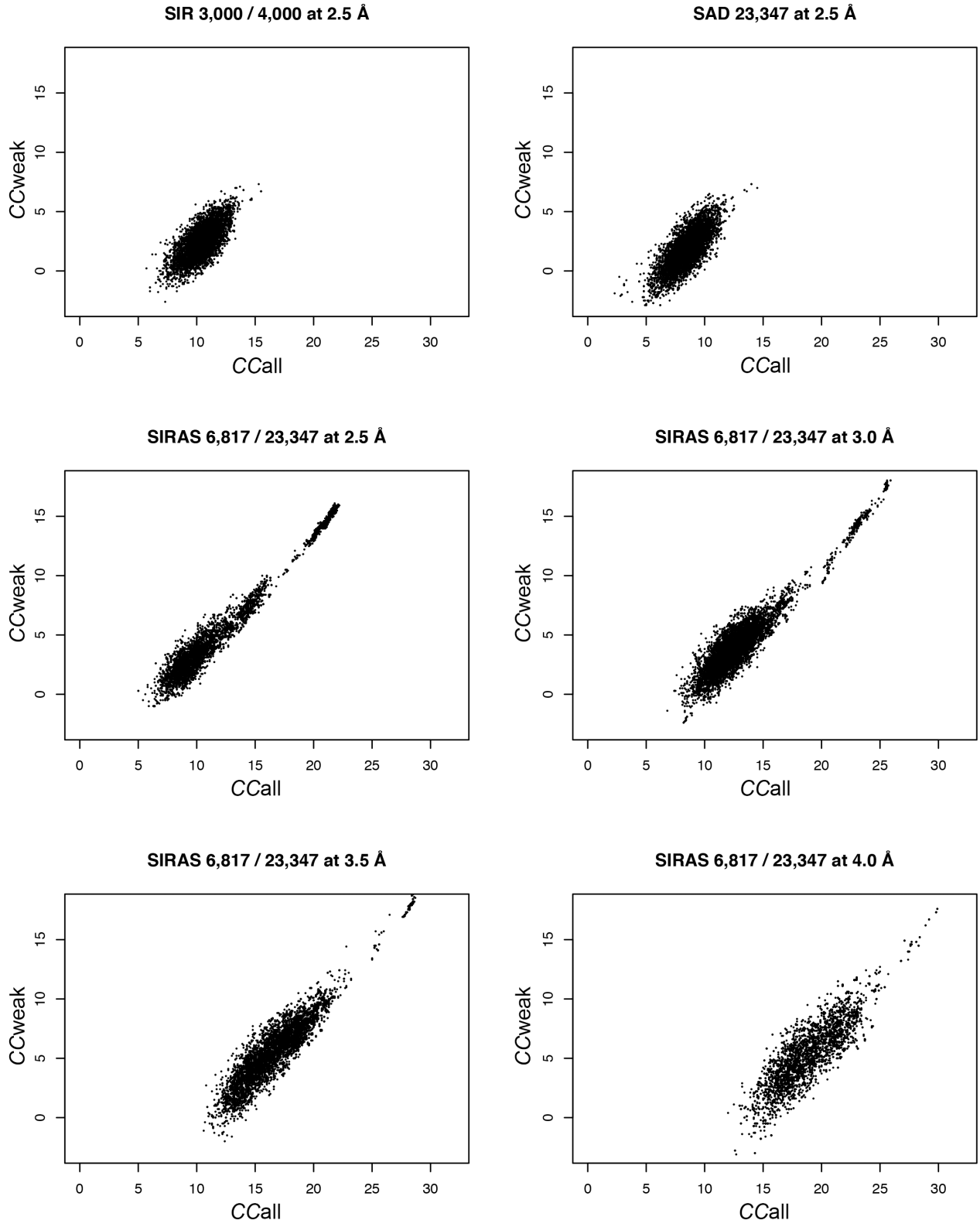

Fig. S4. Scatter plots of CC_{all} and CC_{weak} for *SHELXD* trials. The numbers of indexed images from the native and the derivative datasets are indicated with the phasing method and the high resolution cutoff.

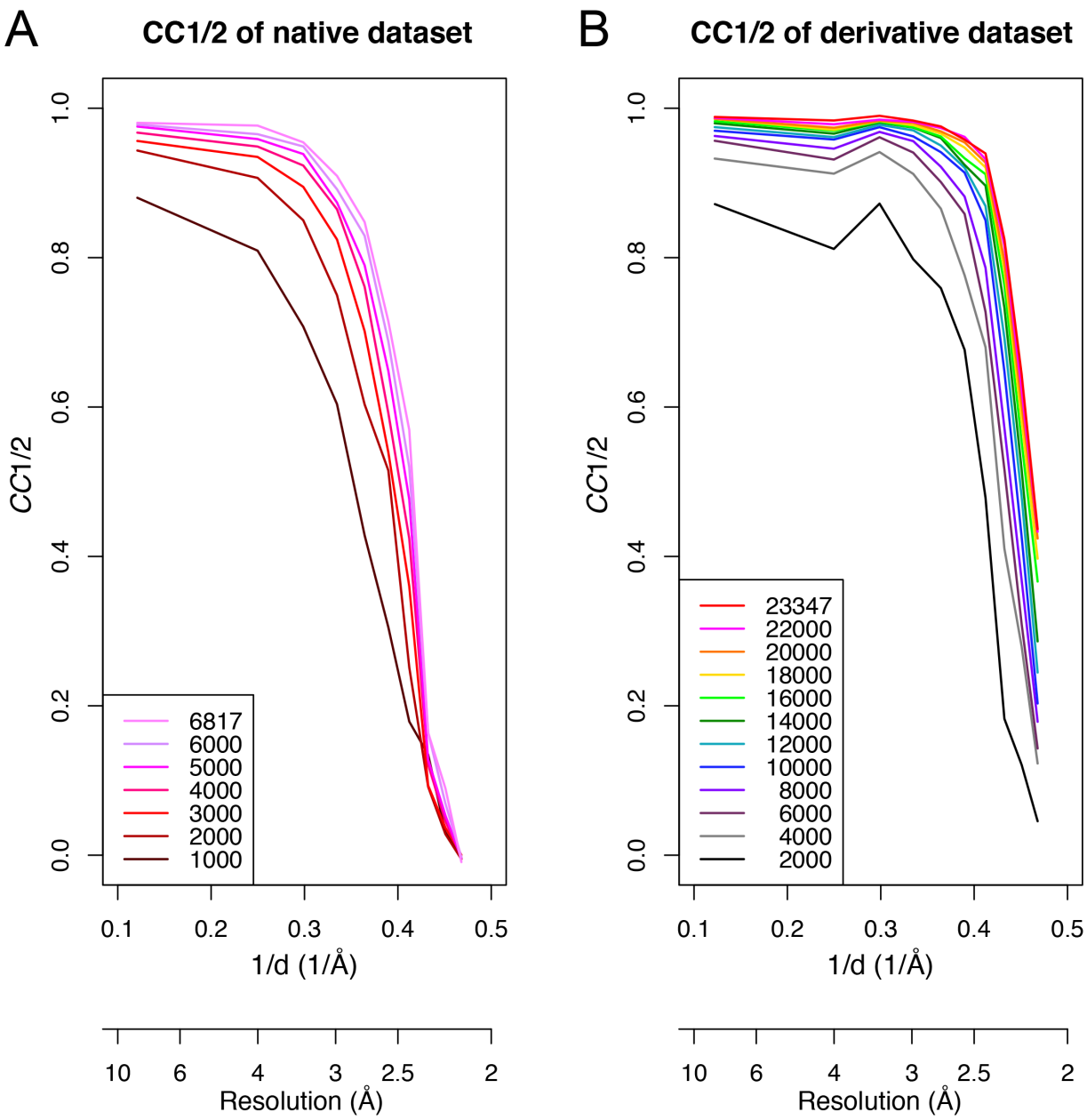

Fig. S5. $CC_{1/2}$ of the native (A) and the HAD13a-derivative (B) bR datasets for different numbers of indexed images.

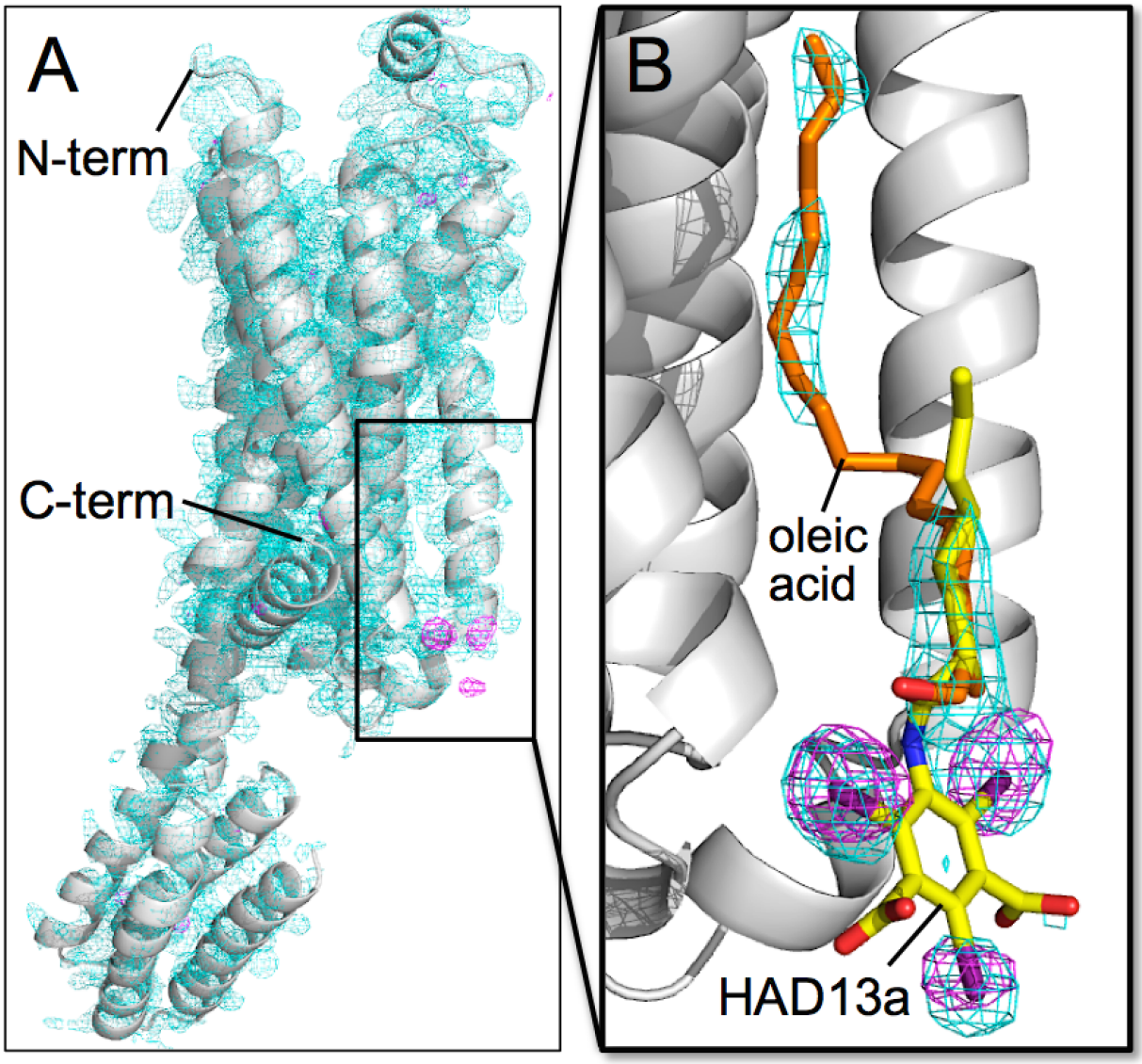

Fig. S6. Successful derivatization of A2a-BRIL with HAD13a. The SFX structure of A2a-BRIL was solved by the molecular replacement method, because I-SAD phasing failed. The final refined structure (gray ribbon model) with $2mF_o - DF_c$ (cyan mesh; 1.0 σ) and anomalous difference (purple mesh; 3.1 σ) maps are shown. (A) Overall structure. (B) Close-up view of the HAD13a binding site. The C, N, O and I atoms of HAD13a (stick models) are colored yellow, blue, red and purple, respectively. An oleic acid (monoolein) molecule is depicted by an orange stick model.

3. SI Table

Table S1. Data collection and refinement statistics for HAD13a-derivatized A2a-BRIL, calculated for datasets merged with Friedel's law, except for CC_{ano}.

Dataset name	A2a-BRIL-HAD13a
Data collection	
XFEL wavelength (Å)	1.771
Space group	$C222_1$
Unit cell parameters *a, b, c* (Å)	40.19, 179.52, 142.13
Beamtime used (min)	210
No. of collected images	323,452
No. of hits	15,518
No. of indexed patterns	14,877
Indexing rate from hits (%)	93.2
Indexed pattern nos. used	14,877
No. of total reflections	4,093,018
No of unique reflections	23,508
Multiplicity	174.1 (124.8)
Resolution range (Å) (outer shell)	50.0–2.30 (2.38–2.30)
Completeness (%)	100 (100)
R_{split} (%)	9.23 (63.1)
$CC_{1/2}$ (%)	98.9 (65.8)
CC_{ano} (%)	-1.49 (-0.97)
$\langle I/\sigma(I)\rangle$	7.22 (1.76)
Refinement	
No. of reflections	22,310
R_{work} / R_{free} (%)	16.5 / 22.9
Mean *B*-factor (Å^2)	71.8
No. of non-H atoms	3,571
Rmsd from ideal bond lengths (Å) / angles (°)	0.016 / 2.008

4. SI References

1. Aguiar J, Carpena P, Molina-Bolivar JA, & Ruiz CC (2003) On the determination of the critical micelle concentration by the pyrene 1 : 3 ratio method. *J Colloid Interf Sci* 258(1):116-122.
2. Oesterhelt D & Stoeckenius W (1974) Isolation of the cell membrane of Halobacterium halobium and its fractionation into red and purple membrane. *Methods Enzymol* 31:667-678.
3. Sugahara M*, et al.* (2015) Grease matrix as a versatile carrier of proteins for serial crystallography. *Nature methods* 12(1):61-63.
4. Weierstall U*, et al.* (2014) Lipidic cubic phase injector facilitates membrane protein serial femtosecond crystallography. *Nature communications* 5:3309.
5. Ishikawa T*, et al.* (2012) A compact X-ray free-electron laser emitting in the sub-angstrom region. *Nature Photonics* 6(8):540-544.
6. Kameshima T*, et al.* (2014) Development of an X-ray pixel detector with multi-port charge-coupled device for X-ray free-electron laser experiments. *Rev Sci Instrum* 85(3):033110.
7. Tono K*, et al.* (2015) Diverse application platform for hard X-ray diffraction in SACLA (DAPHNIS): application to serial protein crystallography using an X-ray free-electron laser. *Journal of synchrotron radiation* 22(Pt 3):532-537.
8. Nakane T*, et al.* (2016) Data processing pipeline for serial femtosecond crystallography at SACLA. *Journal of Applied Crystallography* 49:1035-1041.
9. Huang KS, Bayley H, & Khorana HG (1980) Delipidation of bacteriorhodopsin and reconstitution with exogenous phospholipid. *Proc Natl Acad Sci U S A* 77(1):323-327.
10. Liu W*, et al.* (2012) Structural basis for allosteric regulation of GPCRs by sodium ions. *Science* 337(6091):232-236.
11. Mancusso R, Karpowich NK, Czyzewski BK, & Wang DN (2011) Simple screening method for improving membrane protein thermostability. *Methods* 55(4):324-329.
12. Hattori M, Hibbs RE, & Gouaux E (2012) A Fluorescence-Detection Size-Exclusion Chromatography-Based Thermostability Assay for Membrane Protein Precrystallization Screening. *Structure* 20(8):1293-1299.
13. Caffrey M & Porter C (2010) Crystallizing membrane proteins for structure determination using lipidic mesophases. *J Vis Exp* (45).
14. Joti Y*, et al.* (2015) Data acquisition system for X-ray free-electron laser experiments at SACLA. *Journal of synchrotron radiation* 22(Pt 3):571-576.
15. Barty A*, et al.* (2014) Cheetah: software for high-throughput reduction and analysis of serial femtosecond X-ray diffraction data. *J Appl Crystallogr* 47(Pt 3):1118-1131.
16. White TA*, et al.* (2013) Crystallographic data processing for free-electron laser sources.

Acta crystallographica. Section D, Biological crystallography 69(Pt 7):1231-1240.

17. Duisenberg AJM (1992) Indexing in Single-Crystal Diffractometry with an Obstinate List of Reflections. *Journal of Applied Crystallography* 25:92-96.
18. Zaefferer S (2000) New developments of computer-aided crystallographic analysis in transmission electron microscopy. *Journal of Applied Crystallography* 33:10-25.
19. McCoy AJ*, et al.* (2007) Phaser crystallographic software. *J Appl Crystallogr* 40(Pt 4):658-674.
20. Emsley P, Lohkamp B, Scott WG, & Cowtan K (2010) Features and development of Coot. *Acta crystallographica. Section D, Biological crystallography* 66(Pt 4):486-501.
21. Murshudov GN*, et al.* (2011) REFMAC5 for the refinement of macromolecular crystal structures. *Acta crystallographica. Section D, Biological crystallography* 67(Pt 4):355-367.
22. Winn MD*, et al.* (2011) Overview of the CCP4 suite and current developments. *Acta crystallographica. Section D, Biological crystallography* 67(Pt 4):235-242.
23. Thorn A & Sheldrick GM (2011) ANODE: anomalous and heavy-atom density calculation. *J Appl Crystallogr* 44(Pt 6):1285-1287.
24. VanAken T, Foxall-VanAken S, Castleman S, & Ferguson-Miller S (1986) Alkyl glycoside detergents: synthesis and applications to the study of membrane proteins. *Methods Enzymol* 125:27-35.